Intraseasonal to interannual variations of the temperature structure around the tropical tropopause and their relationships with convective activities

Eriko Nishimoto and Masato Shiotani

Research Institute for Sustainable Humanosphere (RISH), Kyoto University, Japan.

eriko@rish.kyoto-u.ac.jp shiotani@rish.kyoto-u.ac.jp

1. 100hsPa Temperature Structure

Low temperatures generally occur over the equator and extend north-west and south-west in the subtropics to form the **horseshoe-shaped structure**, especially during the northern and southern summers (Fig. 1).

The horseshoe-shaped temperature structure resembles the stationary wave response to tropical heating, which is known as the Matsuno-Gill pattern (Fig. 2). However, the quantitative evaluation of its relationship with convective activities are not clear yet.

Convective activities are present adjacent to monsoon regions during the northern and southern summers. During the northern summer, convective activities occur two monsoon areas with different variability [*Murakami and Matsumoto*, 1994].

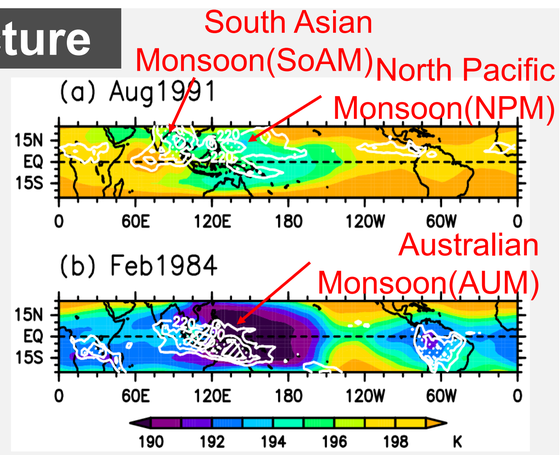

Fig. 1: Maps of temperatures at 100 hPa and OLR at (top) August 1991 and (bottom) February 1984.

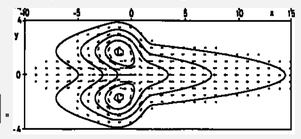

Fig. 2: Idealized Matsuno-Gill pattern [*Gill* 1980].

2. Data

- Temperature@100hPa: ERA-40 monthly data / ERA-interim daily data
- Outgoing Longwave Radiation (OLR) as a proxy of deep convection
- Southern Oscillation Index (SOI) to assess the ENSO effect

3. Definition of Indices

First, two preliminary indices are defined as follows:

- **HSI-R** (Representative of the Rossby response)

$$\mathrm{HSI\text{-}R}(x,t)=\frac{T(10°\mathrm{N}\text{-}15°\mathrm{N})+T(10°\mathrm{S}\text{-}15°\mathrm{S})}{2}-\mathrm{Teq}$$

- **HSI-K** (Representative of the Kelvin response)

$$\mathrm{HSI\text{-}K}(x,t)=\mathrm{Teq}(x+10°,t)-\mathrm{Teq}(x-10°,t)$$

Fig. 4 reveals that negative values of HSI-R and HSI-K are present in the Eastern Hemisphere, especially during the northern and southern summer.

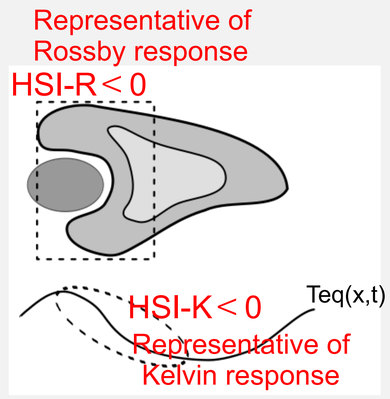

Fig. 3: A schematic diagram of the horseshoe-shaped structure.

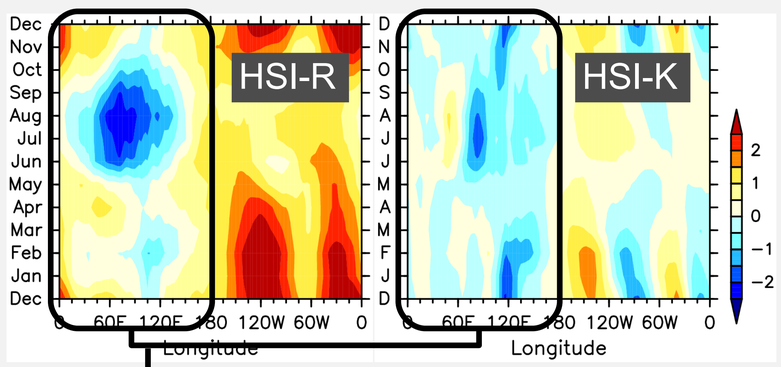

Fig. 4: Longitude–time sections of (left) HSI-R and (right) HSI-K averaged over 23 years.

4. Integrated Index

HSI-1 is integrated from a positive linear relation between HSI-R and HSI-K. This was derived by the first basis function of an empirical orthogonal function (EOF) analysis with HSI-R and HSI-K in the Eastern Hemisphere (Fig. 5).

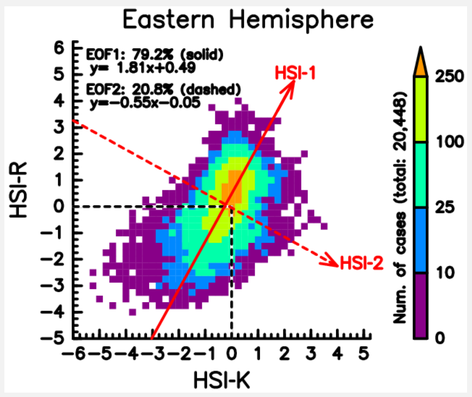

Fig. 5: Frequency of occurrence for HSI-K and HSI-R in the Eastern Hemisphere.

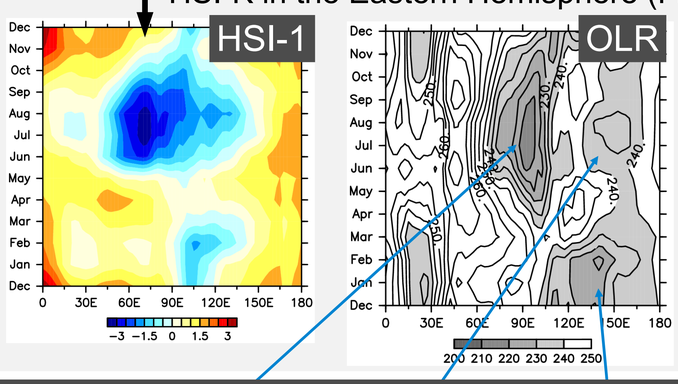

Fig. 6: Longitude–time sections of climatological (left) HSI-1 and (right) OLR.

5. Seasonal Variability adjacent to Monsoon Regions

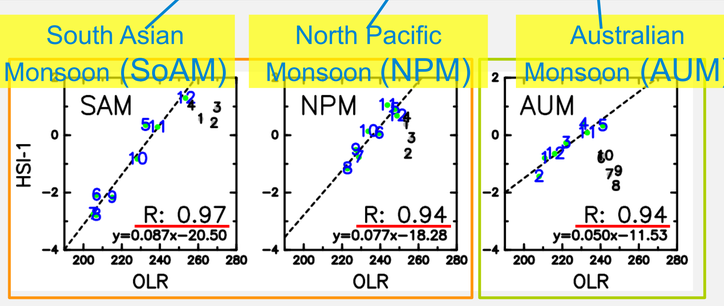

Fig. 7: Scatterplots of climatological OLR and HSI-1 values in the (left) SoAM, (middle) NPM and (right) AUM domains.

From Fig.6, low OLR values occur adjacent to three monsoon regions: South Asian Monsoon (SoAM) and North Pacific Monsoon (NPM) during the northern summer and Australian Monsoon (AUM) during the southern summer. Seasonal cycle in HSI-1 is significantly related to that in OLR values adjacent to these monsoon regions (Fig. 7).

6. Interannual Variability

6-1. Northern Summer

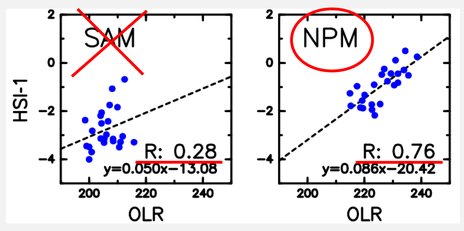

Fig. 8: Scatterplots of OLR and HSI-1 values averaged over July–August in the (left) SoAM and (right) NPM areas.

In the NPM domain, interannual variation in the HSI-1 values is related to that in the OLR values (Fig. 8), associated with the ENSO cycle with about a half-year time lag (not shown), consistent with *Kawamura et al.,* [1998].

In the SAM domain, interannual variation in the HSI-1 values is not related to that in the OLR values (Fig. 8). It is mainly controlled by isolated high temperatures, which are surrounded by the horseshoe-shaped temperature structure. The HSI-1 values vary associated with the ENSO cycle, consistent with *Nishi et al*.'s [2010] previous study on the warm anomaly,

6-2. Southern Summer

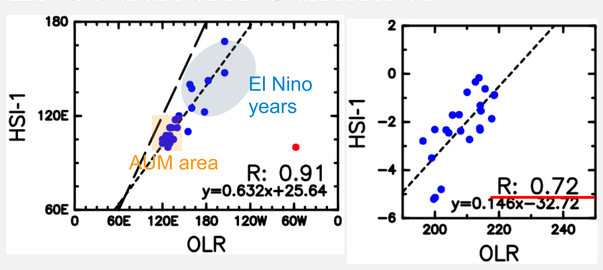

(Left) Fig. 9: A scatterplot of longitude of OLR and HSI-1 minima in each year during January–February.
(Right) Fig. 10: Same as Fig. 10, but for values of OLR and HSI-1 minima.

Fig. 9 reveals that the longitudinal phase difference between HSI-1 and OLR is large as the minima shifts eastward. There is a positive relation between the OLR and HSI-1 minima (Fig. 10). The years when the HSI-1 minimum is nearly zero are in El Nino phase, and the horseshoe-shaped structure is present around the dateline (not shown).

7. Intraseasonal Variability during the Southern Summer

7-1. Cluster Analysis of ISO events

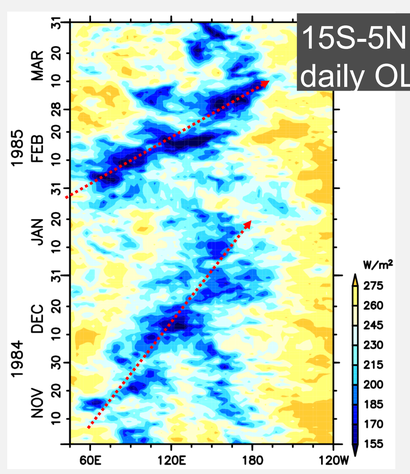

Fig. 11: Longitude-time section of the unfiltered OLR (15S-5N) for Nov-Mar 1984/85.

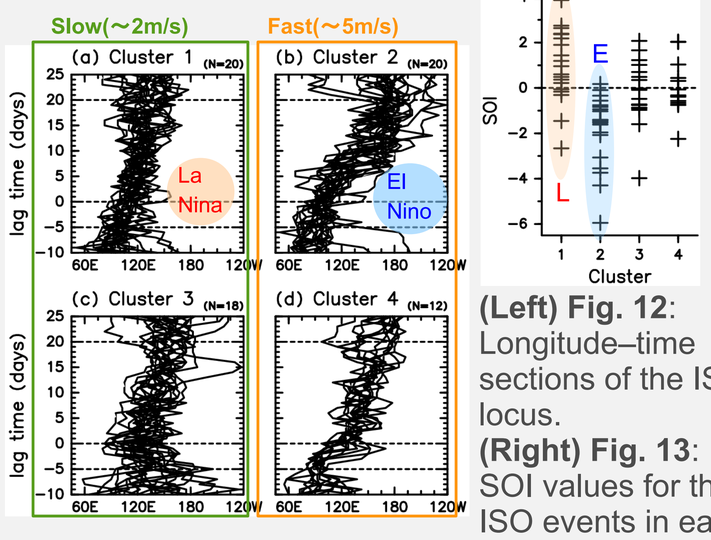

(Left) Fig. 12: Longitude–time sections of the ISO locus.
(Right) Fig. 13: SOI values for the ISO events in each cluster.

As seen in Fig. 11, convective activities observed in the unfiltered OLR field have various types of the eastward propagation features associated with the ISO. By performing cluster analysis using the locus of convective activities, the 72 ISO events selected from 1979–2011 are grouped into Clusters 1–5, which contain 20, 20, 18, 12, and 2 events, respectively (Fig. 12 for the top four clusters). Most of events in Clusters 1 and 2 occur during La Nina and El Nino periods, respectively, and those in Clusters 3 and 4 during weak El Nino (neutral ENSO) periods (Fig. 13).

7-2. Characteristics of each ISO Cluster

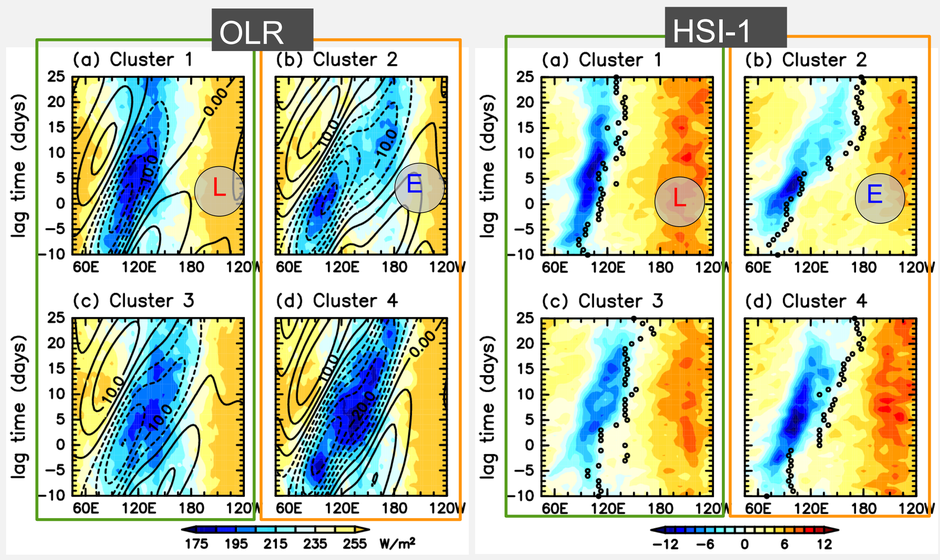

(Left) Fig. 14: Longitude–time sections of the composite unfiltered OLR (color) and band-pass-filtered OLR (contours).
(Right) Fig. 15: Same as Fig. 14, but for HSI-1. Open circles show the convection centers.

The convective activities have a speed of about 2 m/s while propagating to around 120°E and 135°E in Clusters 1 and 3, respectively, and those in Clusters 2 and 4 have a speed of about 5 m/s while propagating eastward into the central Pacific, especially those in Cluster 2 passing over the date line (Fig. 14). During the neutral ENSO periods (Clusters 3 and 4) the propagation speed is faster in Cluster 4 than that in Cluster 3 while the SSTs over the western Pacific are higher in Cluster 4 than those in Cluster 3 (not shown).

Variation in the HSI-1 values are significantly correlated with those in the unfiltered OLR values with both the ISO life cycle (Fig. 15) and event-to-event (not shown).

We found that the strength and location of the minimum temperature at 100 hPa differ among the four clusters (not shown). This implies that different MJOs have different impacts depending on their types.

8. Summary

This study has established the index representing the horseshoe-shaped temperature structure in the tropical tropopause. This index reveals the relaionship to the convective activities adjacent to the monsoon regions in association with the seasonal and interannual time scales, and the relationship to the eastward-propagating convection in associated with the ISO during the southern summer. Cluster analysis is performed according to the ISO propagation features of convective activities observed in the daily OLR field.

The results clearly confirm that the horseshoe-shaped temperature structure is induced by the heating generated by the convective activities.

Secs. 1-6 are published in Nishimoto and Shiotani [2012], *J. Geophys. Res.,* 117, D02104. and Sec. 7 in Nishimoto and Shiotani, *J. Geophys. Res.*, submitted.

Refs.; Gill [1980], *Q. J. R. Meteorol. Soc.*; Kawamura et al. [2001], *J. Meteor. Soc. Jpn.*; Murakami and Matsumoto [1994], *J. Meteor. Soc. Jpn.*; Nishi et al. [2010]. *J. Geophys. Res.*